Proceedings of the ASME 2009 2nd Micro/Nanoscale Heat & Mass Transfer International Conference
MNHMT2009
December 18-21, 2009, Shanghai, China

MNHMT2009-18249

REVISITING THE THERMAL CONDUCTIVITY OF NANOPOROUS MATERIALS

Chandan Bera[1,2], Natalio Mingo[1], and S. Volz[2]

[1]CEA, LITEN, 17 rue des Martyrs, BP166, 38042 Grenoble, France
[2]Laboratoire dEnergetique Moleculaire et Macroscopique, CNRS UPR 288, Ecole Centrale Paris, France

ABSTRACT

Although the thermal conductivity of nanoporous materials has been investigated in the past, previous models have overestimated the small pore limit. Various authors had proposed a cylindrical boundary geometry to mimic the pore's environment. This permits to solve the phonon Boltzmann equation analytically [1]or numerically [2], but for fixed porosity it leads to a saturation of the thermal conductivity at small pore diameters. We show that such saturation is a spurious effect of the cylindrical boundary approximation. By implementing a Monte Carlo calculation with correct boundary conditions, we obtain considerably different thermal conductivities than predicted by the cylindrical boundary geometry. The approach is illustrated in the case of Si and SiGe nanoporous materials.

1 INTRODUCTION

In many recent publications Ref. [3–7], we have seen that nano structuring of bulk material can reduce the thermal conductivity that can increase the figure of merit, ZT of the material. The figure of merit is $ZT = S^2\sigma T/\kappa$, where S Seebeck coefficient,σ electrical conductivity and κ is the thermal conductivity.There has been enormous research in this direction to develop new thermo electric material with a low value of thermal conductivity. Nano and Micro structure base material such as superlattice and quantum dot superlattice have shown significant reduction in thermal conductivity values compared to their bulk values. Nanocomposite porous material can also reduce the thermal conductivity and enhance the nano scale effects observed in supperlattice [1,2,8–10]. In the Ref. [1,2],We have seen theoretical study on periodically aligned nanoporous composite material. In fact these model have over simplified some of the dependencies due to their boundary condition on their model. A Monte Carlo Simulation for periodically aligned cylindrical nano pores inside a host matrix shows that thermal conductivity is strongly decreased with the decrement of the pore radius. Here We have also noticed that thermal conductivity of nano porous alloy material behaves different way than the non alloy porous materials. Recently we have seen some experimental effort and advance in the synthesis of nanostructured semiconductor. Chen et al [11, 12] demonstrated that n-type and p-type SiGe bulk alloy can enhance the figure of merit due to their decrement in the thermal conductivity. Porous material will play a bigger role due to their low thermal conductivity. All those applications where very low thermal conductivity is essential, porous composite material can be very useful [13–15].

In nanoporous composite material the characteristic dimension d is comparable to the mean free path(Λ) of the heat carrier; therefore the heat transport becomes affected by the pore size and pore arrangement. In such a case, heat conduction model known as Fourier law becomes invalid. In literature, the approaches used for the nanoporous composite material are based on the solution of the Boltzmann transport equation for phonons. BTE has been used to model the thermal conductivity of porous silicon constituted of cylindrical pores. The thermal conductivity in the cylinder longitudinal direction was predicted by Yang and Chen [2] using the DOM, while perpendicular to the cylinder surface was simulated by Prasher [16] using the Loyalka's variational method [17]. In these models, the two dimensional(2D) heat transport is considered. Here we used Monte Carlo simulation method for the phonon transport through a three dimensional(3D) array of parallel pores.

2 MONTE CARLO SIMULATION

Monte Carlo simulation technique has been widely used to solve the transport equation. In this technique we can easily follow different scattering processes, such as phonon phonon scattering, phonon particle scattering, and boundary scattering [18–20]. For our Monte Carlo simulation of the cylindrical parallel pores in side a host matrix, we consider a unit cubic cell surrounding the cylindrical pore Fig.1(e). This simulation is frequency independent. we launch phonons from the one square wall and calculate the flux in the opposite wall. Before launching the phonon we define some initial conditions.

2.1 Position:

we arbitrarily choose the position of each phonon inside the square wall and out side the inner circle, Fig.1.(c).

2.2 Velocity:

Each phonon we gave a random velocity in three dimension(3D). For the direction of the phonon we consider Cartesian coordinate, so we defined three random number. As we were launching phonon from the wall so two random number are between -1 to 1 and one random number which define the direction along the pores length is between 0 and 1.

2.3 Free Path:

Before launching the phonon from the wall, we define the free path(free flight) length of each phonon from the probabilistic equation $s = -lnRs \times \Lambda_0$ [21]. Where Λ_0 is the mean free path of the bulk and Rs is the random number between 0 and 1.

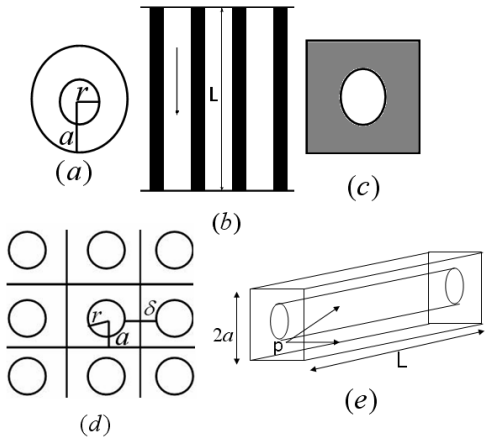

Figure 1. (a) Previous model considering cylindrical outer surface surrounding the pores. (b) Top look of the periodic cylindrical pores inside a host matrix. Phonon transport is directed towards the length of the cylinder. (c) Phonon are launched from the shaded area of the wall. (d) Periodic arrangement of the cylinder. We took Periodic boundary condition on outer surface and diffusive boundary condition on inner pore surface. (e) Pores embedded in a host medium, described geometry we used for numerical simulation.

2.4 Boundary condition:

For the Monte Carlo simulation boundary condition is very important. We put a periodic boundary condition on the four side of cube surrounding the cylindrical pore. For the boundary of the cube we use Cartesian coordinate and for the cylindrical pore we used cylindrical coordinate.

2.5 Scattering:

We consider diffusive boundary condition on the cylindrical pores surface. So if phonon collide with the cylinder, its scattered diffusively in all direction outside the cylinder with a new free path(s). If the phonon cross any of the four surface of the cube surrounding the pore, we again inject a phonon from the opposite side with same velocity and with the remaining free path. If the free path is less than the length(L), then after the traveled distance we generate a new phonon with new velocity and new free path(s).

2.6 Length:

Length(L), Fig.1(b), of the system should be long enough such that we can achieve the diffusive type dependence of the mean effective free path(Λ) of the system. The number of phonon(N), which are launched from the one side after evolving the whole length when come out through the other side, we

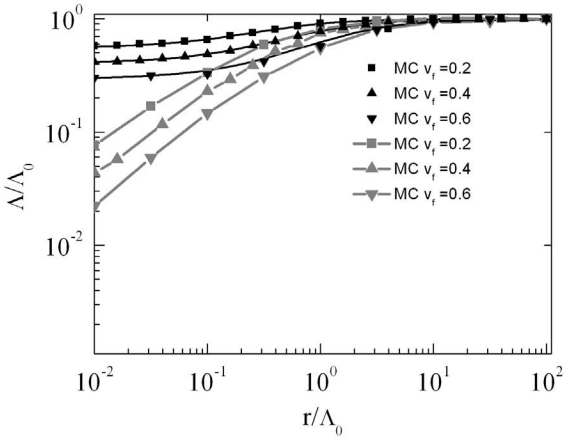

Figure 2. a)Comparisons of the non dimensioned mean free path between the numerical model with periodic boundary conditions using MC simulation(gray line with solid symbol), cylindrical geometry model based on analytical (black line) and MC (symbol) predictions for $v_f = 0.2, 0.4 and 0.6$.

can define the mean effective free path, Λ as

$$N_{through}/N \simeq \left(1+L/\Lambda\right)^{-1}. \tag{1}$$

Where $N_{through}$ is the number of transmitted phonon.

In our simulation we used 10^6 number of phonon and the L was made to vary upto $10^{0.7} \times \Lambda_0$, until we had a good accuracy($\geq 99\%$). To verify our model, we first simulate the phonon effective mean free path for the previous cylindrical model as shown in Fig.1.(a) and we got the same result as the previously predicted Fig.2.

Here we have computed the Mean free path reduction due to the presence of the pore, Λ/Λ_0. Only three independent parameters are involved: the bulk mean free pathΛ, the pore radius r, and the porosity v_f. The inter pore distance, δ is related to the pore radius and porosity as $\delta = 2r((0.5/\sqrt{\frac{v_f}{\pi}})-1)$. Fig.2 shows that mean free path decrease with the decreasing of pore radius, contrary to the previously calculated cylindrical model [1], no saturation occurs at small pore size.

The mean free path keep decreasing as the the pores becomes smaller because for a fixed porosity when we decreased the pores radius, we also increase the density of pores inside the medium and decreased the inter pore distance. So there is more diffusive scattering by the pores and the phonon effective mean free path decreased depending on the inter pore distance.

3 EQUATION FOR THE THERMAL CONDUCTIVITY

In the relaxation time approximation, the thermal conductivity can be expressed as [22]

$$\kappa = \frac{k_b^4}{2\pi^2 v\hbar^3} T^3 \int_0^{xc} \tau \frac{x^4 e^x}{(e^x-1)^2} dx \tag{2}$$

Where τ is the relaxation time, x stands for $\hbar\omega/k_B T$, v is the averaged speed of sound. Now if the relaxation time only depend on the frequency, we can define

$$\tau(\omega) = \frac{\Lambda(\omega)}{v} \tag{3}$$

Now we can use the result of Monte Carlo simulation to compute the $\Lambda(\omega)$. In the Monte Carlo simulation we have Λ/Λ_0 frequency independent, but it depend on the zero porosity mean free path of bulk Λ_0, pore size r, and porosity v_f, so, $\frac{\Lambda}{\Lambda_0} = F(\Lambda_0, r, v_f)$. The zero porosity mean free path, i.e., the bulk mean free path of the matrix can be expressed as a frequency dependent form [23]

$$\Lambda_0(\omega) = v(BT\omega^2 e^{-C/T})^{-1} \tag{4}$$

Where B and C are two parameters. In this Anharmonic scattering procedure both umklapp and normal scattering processes are included. For the higher frequency, umklapp scattering is proportional to ω^2, and it thus dominate over normal processes which depend linearly on frequency [24]. This justifies the form of $\Lambda_0(\omega)$ in Eqn.4. we choose the same value of constant B and C as Ref. [23]. We employed this approach for the thermal conductivity calculation of pure Si. Therefore the effective frequency dependent mean free path of phonon for porous Si became

$$\Lambda(\omega) = \Lambda_0(\omega) F(\Lambda_0, r, v_f) \tag{5}$$

For the SiGe alloy we use the effective medium base approached same as Ref. [25]. $\Lambda_0(\omega)$ in this expression is combination of the average anharmonic scattering rate of bulk Si and bulk Ge with the alloy scattering term of SiGe, first introduced in Ref. [26]. So for the SiGe alloy the effective mean free path became

$$\Lambda(\omega) = \frac{1}{\frac{1}{\Lambda_0(\omega)F(\Lambda_0,r,v_f)} + \alpha^4\omega^4} \tag{6}$$

where α is due to the atomic disorder in alloy and it proportional to the volume fraction of Ge in the SiGe alloy.

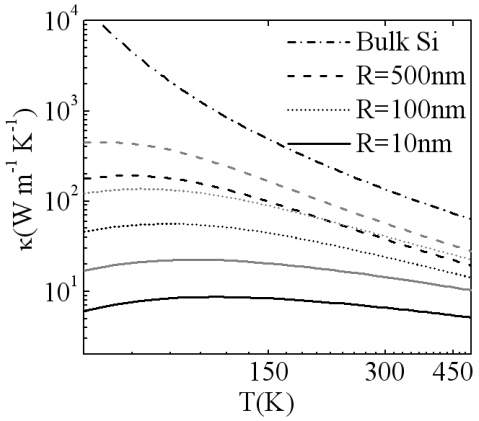

Figure 3. Thermal conductivity of porous Si at 20% and 40% porosity for different pores radius. Black line is for 40% and gray line is for 20% porosity.

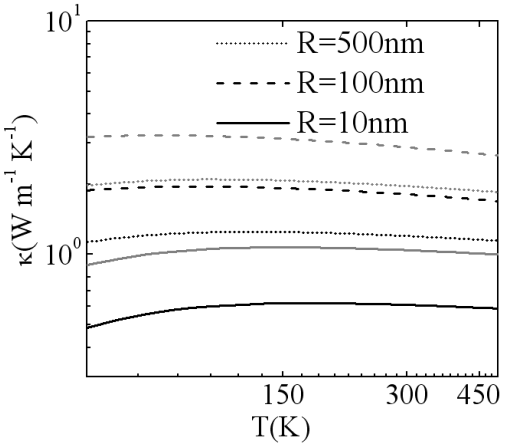

Figure 4. Thermal conductivity of porous $Si_{0.8}Ge_{0.2}$ at 20% and 40% porosity for different pores radius. Black line is for 40% and gray line for 20% porosity.

4 RESULTS

Using the Eqs.2, 5 and 6 we can study the dependence of thermal conductivity on the temperature for different porosity and pore radius. As shown, in Fig.3, from Eqs.2, 5 we see that the thermal conductivity of porous Si is lower than the thermal conductivity of bulk material and as we increase the porosity the thermal conductivity decreased. On the other hand, in the Fig.4, from Eqs. 2, 6 we see that the thermal conductivity of porous SiGe alloy is not affected by the pore at all temperature range. It remains almost temperature indeependent.

Here we report the thermal conductivity on the term of temperature. Since in the alloy smaller wave length phonon is scattered by the atomistic disorder, the longer wave length phonon is responsible for heat transport. So very large size of pores are also able to block a significant amount of phonon. But in the non alloy material, larger frequency range carry the heat and although long wave length phonon is blocked by the pores size, a significant heat come from the short wave length phonon. The effect of pores size on the thermal conductivity of alloy and non alloy material was discussed in detail in another paper.

5 CONCLUSION:

We report the three dimensional (3D) heat transport for porous alloy and non alloy material. We found that porous alloy material is more effective to reduce the thermal conductivity than non alloy materials. Using Monte Carlo simulation we also improved the effective mean free path of the material for lower pores size. In $Si_{0.8}Ge_{0.2}$ alloy, at 300K we see that thermal conductivity is nearly 5 times and 3 times smaller than the bulk thermal conductivities value for 20% porositi at 100nm and 500 nm pores radius respectively. Though Ge have limited resources and it is not cheap material, still the SiGe alloy with a very low percentage of Ge can be used to reduce thermal conductivity very effectively. So the application where the low thermal conductivity is important, porous alloy material can be very advantageous [28, 29]. The difficulty of fabrication of nano size pores may be an obstacle for this kind of materials. Porous alloy will allow to take advantage of the large pore size which will be easier to produce.

ACKNOWLEDGMENT

We acknowledge the CNRS, CEA and ANR ThermaEscape for their financial support.

REFERENCES

[1] Ravi Prasher, J. Appl. Phys. **100**, 034307 (2006).
[2] Ronggui Yang,Gang Chen and Mildred S. Dresselhaus, Phys. Rev. B **72**,125418 (2005).

[3] L. D. Hicks and M. S. Dresselhaus, Phys. Rev. B, **47**, 12727 (1993).
[4] G. Chen, Phys. Rev. B 57, 14958 (1998).
[5] R. Venkatasubramanian, E. Siivola, T. Colpitts, and B. O'Quinn, Nature (London) **413**, 597 (2001).
[6] T. C. Harman, P. J. Taylor, M. P. Walsh, and B. E. LaForge, Science **297**, 2229 (2002).
[7] C. M. Bhandari and D. M. Rowe, Contemp. Phys. 21, 219 (1980).
[8] J. D. Chung and M. Kaviany, Int. J. Heat and Mass Transfer **43**, 521 (2000).
[9] J.-H. Lee,J. C. Grossman,J. Reed and G. Galli, Appl. Phys. Lett. **91**, 223110 (2007).
[10] Ronggui Yang and Gang Chen, Phys. Rev. B**69**, 195316 (2004).
[11] X. W. Wang, H. Lee, Y. C. Lan, G. H. Zhu, G. Joshi, D. Z. Wang, J. Yang, A. J. Muto, M. Y. Tang, J. Klatsky, S. Song, M. S. Dresselhaus, G. Chen, and Z. F. Ren, Appl. Phys. Lett. **93**, 193121 (2008).
[12] Giri Joshi, Hohyun Lee, Yucheng Lan, Xiaowei Wang, Gaohua Zhu, Dezhi Wang, Ryan W. Gould, Diana C. Cuff, Ming Y. Tang, Mildred S. Dresselhaus, Gang Chen and Zhifeng Ren, Nano Lett. **8**, 4670 (2008)
[13] A. Drost, P. Steiner, H. Moser, and W. Lang, Sens. Mater. **7**, 111 (1995).
[14] T. M. Kuzay, Rev. Sci. Instrum. **63**, 468 (1992).
[15] A. Delan, M. Rennau, S. E. Schulz, and T. Gessner, Microelectron. Eng. **70**, 280 (2003).
[16] R. Prasher, J. Appl. Phys. **100**, 064302 (2006).
[17] S. K. Loyalka, Int. J. Heat Mass Transfer, **12**, 1513 (1969).
[18] S. Mazumder and A. Majumdar, J. Heat Transfer **123**, 749 (2001).
[19] David Lacroix, Karl Joulain and Denis Lemonnier, Phys. Rev. B **72**, 064305 (2005).
[20] Jaona Randrianalisoa and Dominique Baillis, J. Appl. Phys. **103**, 053502 (2008).
[21] S.Volz(Ed.), Microscale and Nanoscale Heat Transfer(Paris,2005), PP.133-153.
[22] J. Callaway, Phys Rev. **113**,1046 (1959)
[23] N.Mingo,Phys. Rev. B **68**,113308 (2003).
[24] Y.-J. Han and P.G. Klemens, Phys. Rev. B, **48**, 6033 (1993).
[25] N. Mingo, D. Hauser,N. P. Kobayashi,M. Plissonnier and A. Shakouri *Nano lett*, 9(2), (2009).
[26] Abeles, B. Phys. ReV. **1963**, 131, (1906).
[27] N.Mingo, L. Yamg, D. Li, and A. Majumdar, Nano Lett. (2003).
[28] W. Zhang, N. Mingo, and T. S. Fisher1,Phys. Rev. B **76**, 195429 (2007).
[29] D. A. Broido and N. Mingo, Phys. Rev. B **74**, 195325 (2006).